

Growth-Associated Changes in the Periodontal Bone and Molar Teeth of Male Rats

María F García, Hilda Moreno, Alfredo Rigalli, Rodolfo C Puche*

Here we report quantitative data associating periodontal bone variables of young conventional rats with the growth process. The hemimandibles of male rats (IIM/Fm stock, 2 to 15 wk of age.) were excised and submitted to conventional morphologic, radiologic, and histologic evaluation. The length, area, or X-ray absorbance of various regions or structures was measured on digital images of radiographs by using an image-analysis program. The sum of periodontal bone areas undergoing resorption (interproximal + intraradicular) increased until 9 or 10 wk of age and decreased thereafter. Mineral accretion rates and mineral density asymptotes were not significantly different among molars. The mineral density of resorption areas in alveolar bone fitted sinusoidal kinetics, indicative of the 'instability' of the tissue due to its high metabolic activity. Mineral accretion rates and mineral density asymptotes were not significantly different among molars. The proportion of root length within alveolar bone exhibited a biphasic curve (minimum at 5 wk of age), due to differences in the growth rates of variables involved in its calculation (distance between the cemento-enamel junction to the apex and height of the resorption areas). The distance between the cemento-enamel junction and alveolar bone crest over time fitted a sigmoidal function with a point of inflection that did not differ significantly from that of body or mandible dry weight. In summary, the growth process appears to affect periodontal bone support and the distance between the cemento-enamel junction and alveolar bone crest in male rats.

Abbreviation: POI, point of inflection.

Organisms present in microbial dental plaque and the gingival sulcus or substances derived from them are primary agents in the etiology of inflammatory gingival and periodontal disease. However, apical proliferation of the epithelial attachment (junctional epithelium) and loss of alveolar bone in germfree mice were attributed to periodontal bone disease.^{2,3} Other essential features of the disease (such as inflammation) were absent. Subsequent authors concluded that the previously described changes were "physiological growth phenomena and not pathologic alterations observed in germfree mice."¹⁵ This comment prompted us to ask: How does growth affect periodontal processes of colonized (conventional) animals?

Here we report analytical data regarding the dentition and periodontal status of conventional rats 2 to 15 wk of age. To this end we used 4 complementary techniques typically applied to the assessment of experimental periodontal disease. We learned that growth process affect 2 of these parameters (periodontal bone support and the distance between the cemento-enamel junction and the alveolar bone crest) and integrate our findings with information regarding growth and the mechanics of chewing. The most striking periodontal change during this period was a transient phenomenon: the sum of alveolar bone areas undergoing resorption increased until 9 or 10 wk of age and decreased thereafter. We hypothesize that this phenomenon is due to a transient immunologic impairment.

Materials and Methods

The project was approved by the Bioethics Committee of the Medical School of Rosario (Santa Fe, Argentina). The experiments were carried out according to the principles stated in the NIH guide.²⁸

Animals. The facilities belong to the conventional, semiopen type. Young adult rats of both sexes of each line were separated by sex since weaning and housed first in polypropylene cages (32 cm × 24 cm × 10 cm) with wood shavings for bedding. At 70 d of age, they were housed in wire cages (40 cm × 40 cm × 30 cm) at the rate of 6 animals per cage. The rooms had constant temperature (23 ± 3 °C), with a relative humidity of 50 ± 10% and a 12:12-h photoperiod. Cages and bedding were changed twice a week. Tap water and food (pelletized, Cargill Laboratory Chow, Cargill, Argentina) were provided ad libitum.

The base population, named IIM (Instituto de Investigaciones Médicas), was obtained by crossing outbred albino rats brought from Buenos Aires, Argentina, in 1947, the ancestors of which came from Europe in 1917. The IIM rat colony was initiated in 1948 at the Animal Facilities of the Instituto de Investigaciones Médicas of Rosario (IIM), by randomly assigning breeders of the base population to groups to develop lines a through j, which were bred since then through a nonregular system of mating, in harems with 1 male and 4 to 6 female rats. Upward selection of body weight and productivity was performed in every line. About 2 generations were obtained yearly. Inbreeding was achieved by limiting the effective population size.⁹ A few breeders of the lines IIMb, IIMe, IIMα, and IIMc were moved in 1958, 1960, 1972, and 1980, respectively, to the Animal Facilities of the School of Medicine to give rise to the IIM/Fm colony.

In 1964, a wild *Rattus norvegicus* was crossed with an IIM e/Fm female rat, and 2 sublines were developed from the F1 population:

Received: 28 Jan 2009. Revision requested: 02 Mar 2009. Accepted: 27 Apr 2009.
Bone Biology Laboratory, School of Medicine, Rosario National University, Rosario, Argentina.

*Corresponding author. Email: rodolfopuche@gmail.com

a black hooded substrain (designated 'm') and a black one (the 'l' substrain). These lines are currently in their 111th generation of selective breeding. Their inbreeding coefficient is near maximum.⁷ Genetically determined features of the growth of bone mass were studied in IIM m/Fm and in IIM e/Fm rats.¹⁸

Preparation of hemimandibles. Weekly between ages 2 through 15 wk, random male IIM/Fm rats were euthanized by deep ether anesthesia in a fume hood. The hemimandibles were excised, and the right bones underwent processing for histology. The left hemimandibles were submerged for 5 min in boiling water, defleshed, placed in 3% hydrogen peroxide for 24 h, dehydrated and defatted in ethyl alcohol, and dried at 37 °C until their weight stabilized.

Radiographs of hemimandibles. The defleshed left hemimandibles were placed flat on standard dental X-ray film alongside an aluminum step-wedge reference and radiographed (70 kV; 70 mA; focus–film distance, 5 cm; exposure time, 0.8 s). The step-wedge standard was built from aluminum pieces (width, 5 mm; thickness, 1 mm; length, 10 to 40 mm) glued together with cyanocrylate. The step-wedge provided reference areas of 1.5 to 7.0 mg aluminum per square millimeter. The radiographs of the hemimandibles (buccal–lingual projection) and the aluminum standard were scanned (Genius ColorPage-VRG-v2 scanner; Taipei, Taiwan) to obtain the digital images (resolution, 600 dpi).

Bone densitometry. Measurement of bone mineral content was based on a previously published method.¹⁴ The absorbance of X-rays by alveolar bone and the step-wedge standard were measured by using the freeware image-analysis program NIH Image.¹⁹ Development of films was automated.

The main source of error in the technique comes from variation in the current passing through the cathode and affecting the X-ray spectrum. For each X-ray film, the slope of the line generated by dividing the net absorbance of each step of the step-wedge (average absorbance of the step of interest minus background absorbance) divided by the mass of aluminum at the step of interest was calculated (Figure 1 A and B). Films for which the step-wedge standard gave slopes below or above the range of 0.060 to 0.120 absorbance units as a function of milligrams of Al per square millimeter were discarded and X-ray exposures repeated (Figure 1 C).

The absorbances of various steps (thicknesses) of the aluminum step-wedge were compared with those of sections (different thickness) of defatted cortical bovine bone. Aliquots of these sections were incinerated in a muffle furnace at 500 °C for 10 h. The bone mineral density of the incinerated samples was defined as the ratio between the weight of ashes (in milligrams) and the area (in mm²) of the section exposed to X rays. Figure 1 D shows the relationship between the aluminum and bone standards. Bone mineral density (mg/mm²) was calculated as:

$$\text{Bone Mineral density} = 0.6175^{[0.3445 \times \text{mass of Al standard (mg)/mm}^2]}$$

Areas of resorption of alveolar bone (radiolucent foci) at interproximal and intraradicular sites were counted, and their heights and areas were measured by using the NIH Image program.¹⁹

Periodontal bone support. The length of molar root within periodontal bone was measured from the digital images of the radiographs by using NIH Image. The percentage of root length that was within alveolar bone (that is, periodontal bone support) was calculated as

$$[(A - h) / A] \times 100\%,$$

where A is the distance between the cemento-enamel junction and the apex of the root of interest, and h is the height of the resorption area.¹³ Because periodontal bone support was qualitatively the same for all roots, we here present the data corresponding to the distal root of the first molar and the mesial root of the second molar (averaged for each rat), because their prominence in the radiographs helped to reduce measurement errors.

Distance between the cemento-enamel junction and alveolar bone crest. As described previously,¹³ hemimandibles were stained for 1 min in methylene blue (1 g dye/100 mL solution) to mark the cemento-enamel junction. For each root, the distance between the cemento-enamel junction and alveolar bone crest was measured with the aid of a binocular microscope (magnification, 30×; Carl Zeiss, Essingen, Germany) and a measuring scale placed in the ocular. The smallest distance that could be appreciated was 40 μm.

Before measurements were made, hemimandibles were oriented so that buccal and lingual cusps were superimposed. Measurements (in mm) were obtained from the buccal and lingual faces of the 3 molars, along the axis defined by each root. For each molar, the variable is reported as the average of root measurements.

Height of molar crowns. This length was measured on stained hemimandibles, between the cemento-enamel junction and occlusal border of each cusp, on the buccal view for each molar. At any given age, each rat provided 4 to 6 measurements, which were averaged.

Analysis of histologic sections. Once excised, the right hemimandibles were soaked in 4% formaldehyde solution for 1 d. A carborundum disk then was used to make 2 cuts: medial to the first molar and distal to the third. The block comprising the 3 molars and their surrounding hard and soft periodontal tissues were placed for 2 additional days in formaldehyde solution and then transferred to an EDTA solution (5.5 g/dL, pH 7.4) at 37 °C for 6 to 8 wk. After decalcification and paraffinization, the portion of mandible with 3 molars was cut at 5 μm, producing a total of 300 to 350 sections (sagittally oriented) per sample; these sections were mounted on slides and stained with hematoxylin and eosin. Osteoclasts were counted (magnification, ×450; Integrator II eyepiece, Carl Zeiss, Essingen, Germany). This eyepiece superimposes a reticulum of 90,000 μm² with 100 points. Areas of contact (interproximal and interradsular) between teeth and alveolar bone in every tenth section were assessed; the number of osteoclasts per 100,000 μm² was reported.

Statistics and curve-fitting. Data are reported as mean ± SEM, and Student's *t* tests and ANOVA were performed to assess the significance of differences: *P* < 0.05.²³

Several of the variables we studied exhibited a sigmoidal trace. Calculation of the best fit of the data to the Boltzmann sigmoidal equation allowed us to define the following parameters: A₀ (weight or length units), initial value; A_∞ (weight or length units), asymptotic value; POI (weeks), point of inflection; and S, slope (the inverse of the slope of the tangent at POI) such that

$$Y = A_0 + \{(A_\infty - A_0) / (1 + \exp^{[(\text{POI} - \text{weeks}) / S]})\}$$

The use of Boltzmann's equation was prompted by the need to define quantitatively the kinetics of the periodontal processes that fitted this function. A parameter like the POI was used to define whether a process was or was not associated with body growth.

We also used 2 other nonlinear functions to fit the data: 1-component exponential decay,

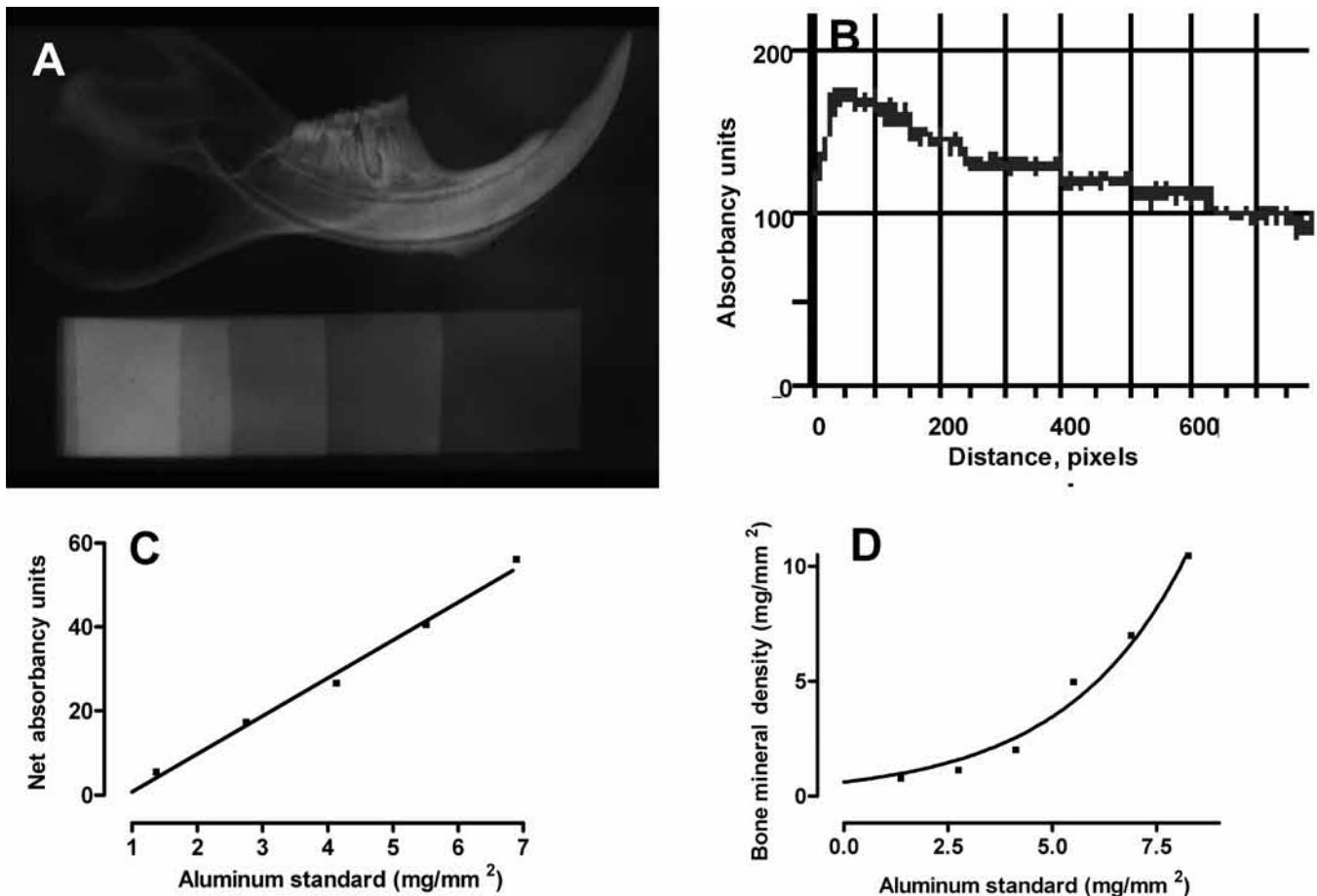


Figure 1. (A) Radiograph of the hemimandible and the step-wedge aluminum standard. (B) Tracing of the absorbancies along the standard. (C) Relationship between the absorbancy units at each step of the standard and its aluminum mass. (D) Relationship between the masses of the aluminum standard and the bone-ash content of cortical bovine bone.

$$Y = Y_0 \times e^{-(kt)},$$

and 1-phase exponential association,

$$Y = Y_{\max} \chi (1 - e^{-kt}).$$

The decay function was used, for example, to fit the distance between the occlusal surfaces and the cementoamel junction as a function of age, whereas exponential association was used to plot the distance from the cementoamel junction to apex or the height of the resorption area as functions of age.

The best fit of the data to a function was performed with the aid of a computer program (GraphPad Prism 2.0, GraphPad Software Inc., San Diego, CA.) whose algorithm proceeds by iterations until the difference between 2 consecutive sums of squares is smaller than 0.01%. To select between 2 different functions, that with the higher R^2 value was chosen.

Results

Comparison of body weight data estimated by using the Parks¹⁷ and Boltzmann equations indicate that both yield similar results regarding the POI (7.0 ± 1.0 versus 6.7 ± 1.05 wk) and asymptote (490 ± 21 versus 417 ± 121 g).

Dentition of young rats. The first and second molars erupted earlier than the third (Figure 2). In agreement with the monophodont character of rodents, the mesiodistal diameter of the molar crowns did not change from 2 to 15 wk of age. The

diameter of crowns of the first, second, and third molars ($n = 43$) measured 2.04 ± 0.01 , 1.40 ± 0.01 and 1.12 ± 0.02 mm, respectively. The diameter of the first molar differed significantly ($P < 0.0001$) from those of the second and third.

The mineral density of the crowns increased as a function of age. The kinetics of mineralization was similar for the first and second molars (Figure 2 A). Although the asymptote of the mineral density of the third molar (6.5 ± 2.5 mg/mm²; Figure 2 B) seems to be greater than those of the first (2.7 ± 0.3 mg/mm²) and second (3.1 ± 0.4 mg/mm²) molars, the differences were not significant.

Periodontal bone support. We present data (averaged for each rat) corresponding to the distal root of the first molar and the mesial one of the second, because the prominence of these roots in the radiographs reduced the likelihood of mistakes during measurement. This variable exhibited a biphasic curve for all molar teeth, with a minimum at the fifth week of age (Figure 3 B).

The 2 variables involved in the calculation of PBS—distance from the cementoamel junction (A) and the height of resorption areas (h)—displayed exponential increases as a function of age with significantly different rate constants (Figure 3 A; for A, $k = 0.34 \pm 0.10$ wk⁻¹; for h, $k = 0.145 \pm 0.018$ wk⁻¹, $P < 0.0001$). These differing constants explain the biphasic character of the curve shown in Figure 3 B.

Increase in the distance from the cementoamel junction to the apex occurred simultaneously with the exponential decay in the growth rate of molar crowns as a function of age, with a time constant of 0.34 ± 0.10 wk⁻¹ (data not shown). Histologic

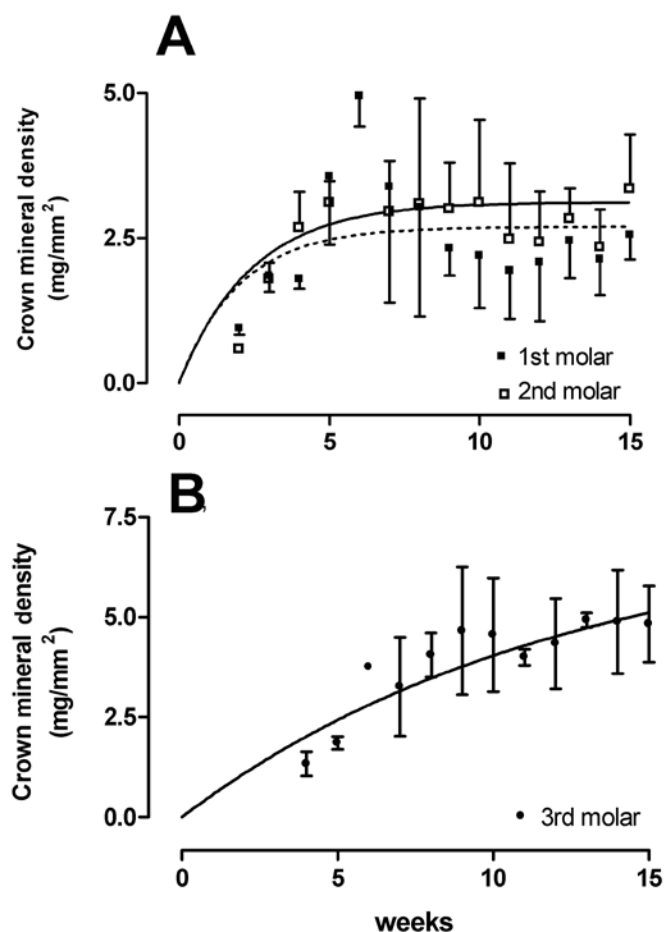


Figure 2. (A) Mineral density of crowns of first and second molars as a function of age. (B) Mineral density of the third molar crown as a function of age. Note that eruption of the third molar occurs at 4 wk of age. Data are given as the mean \pm SE of 4 to 6 animals per point.

evidence (not shown) indicated that active and passive processes of molar eruption were taking place, allowing correct occlusion of molar teeth.

Distance from the cemento-enamel junction to alveolar bone crest. The data from the lingual view of the molars increased along a sigmoidal trace with POIs at 5.7 ± 2.8 , 5.7 ± 0.8 , and 6.5 ± 1.0 wk for the first, second, and third molars, respectively (Figure 4). These POI values did not differ significantly from that of body¹⁸ or mandibular growth: the statistical significance of the comparison of the POI for the first, second, and third molars and that for of body growth (6.7 ± 1.5 wk) was 0.726, 0.292, and 0.858, respectively. The data from the vestibular view were always lower than those from the buccal view and did not converge to the Boltzmann equation.

Rate of mineralization. The rate of mineralization of the hemimandibles followed a sigmoidal trace with a POI at 4.7 ± 0.14 wk and a plateau of 3.16 ± 0.05 mg/mm² at 5 wk or 6 wk of age (Figure 5 C, upper curve).

Transient prepubertal periodontal bone resorption assessed as radiolucent foci. The number of resorption lesions increased with age according to a sigmoidal function with plateaus at 1.9 ± 0.06 wk for interproximal and 3.0 ± 0.16 wk for intraradicular lesions. The POI of these curves occurred at 4.5 ± 0.5 wk (Figure 5 A). Visual inspection of radiographs suggested that the sum of the areas would be a better indicator of this phenomenon. The total area of alveolar bone resorption increased to 9 or 10 wk of age and decreased thereafter (Figure 5 B). The POI occurred at

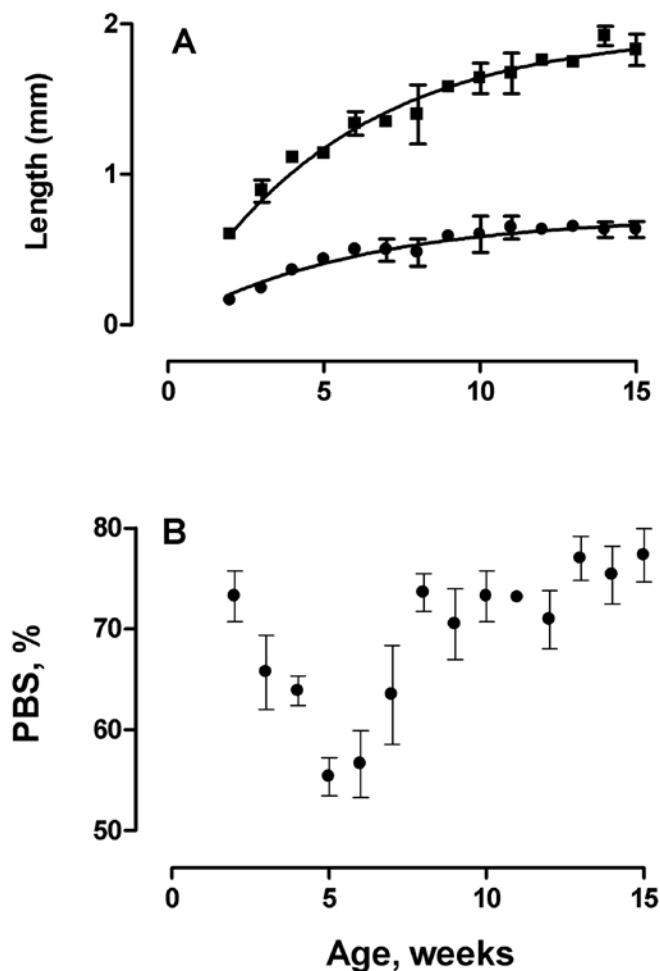


Figure 3. (A) Growth in the length of the distal (first molar) and mesial (second molar) roots (solid squares, averaged for each rat) and height of the adjacent resorption areas (solid circles, averaged for each rat) as a function of age. (B) Periodontal bone support of the distal (first molar) and mesial (second molar) roots (summed and averaged for each rat) as a function of age. Data are given as the mean \pm SE of 4 to 6 animals per point.

4.5 ± 0.6 wk, and the process reached its plateau at 8 to 10 wk, regressing thereafter.

No significant periodontal infiltration with mononuclear cells was noted. The active osteoclastic activity in alveolar bone that was noted could not be attributed to periodontal disease because it occurred during a period of very active bone turnover consistent with the most active period of growth. Osteoclasts counts did not differ significantly between 3 and 9 wk of age (3 wk: $n = 4$, 36 ± 3 osteoclasts /100,000 μm^2 ; 9 wk: $n = 6$, 42 ± 4 osteoclasts /100,000 μm^2).

The average mineral density at the resorption areas of alveolar bone exhibited a sinusoidal course as a function of age, with high goodness of fit ($R^2 = 0.816$). The average mineral density was 1.404 ± 0.035 mg/mm², with an amplitude of 0.317 ± 0.047 mg/mm² (Figure 5 C, lower curve).

Discussion

Here we report quantitative data associating periodontal bone variables with the growth process investigated in young conventional rats. The sum of periodontal bone areas undergoing resorption (interproximal + intraradicular) increased between 3 and 9 to 10 wk of age and decreased thereafter. The osteoclasts counts between 3 and 9 weeks of age, however, showed no

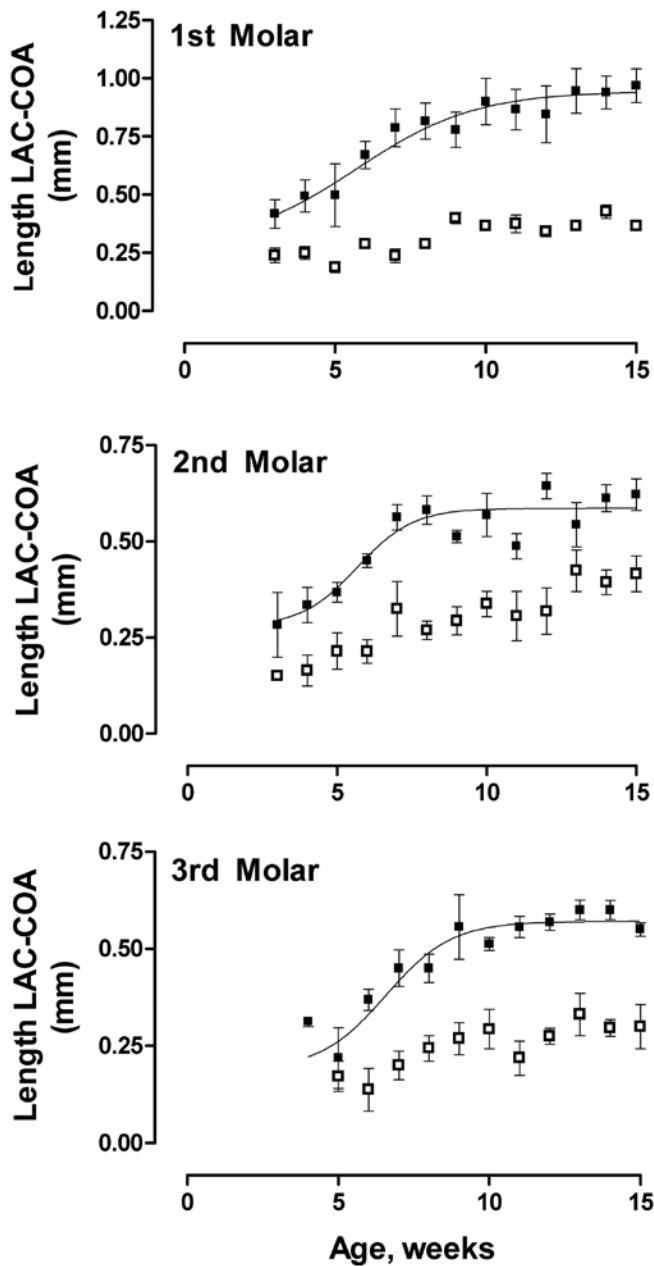


Figure 4. Time course of the length from the cementoamalgam junction to the alveolar bone crest for the first, second, and third molars as a function of age at the lingual (solid squares) and buccal (open circles) surfaces. Data are given as the mean \pm SE of 4 to 6 animals per point.

significant differences. The mineral density of resorption areas in alveolar bone fitted sinusoidal kinetics, indicative of the 'instability' of the tissue due to its high metabolic activity. In addition, periodontal bone support exhibited a biphasic curve due to differences in the growth rates of variables involved in its calculation. Finally, the distance between the cementoamalgam junction and alveolar bone crest in male rats changed as a function of age, in phase with body growth.

Point of Inflection

The POI of a function describing a periodontal process was taken as a criterion to associate that process with body growth. Because an objective of this investigation was to assess the effect of the growth process on the periodontal tissue of control animals, describing the criteria used to achieve that goal is pertinent.

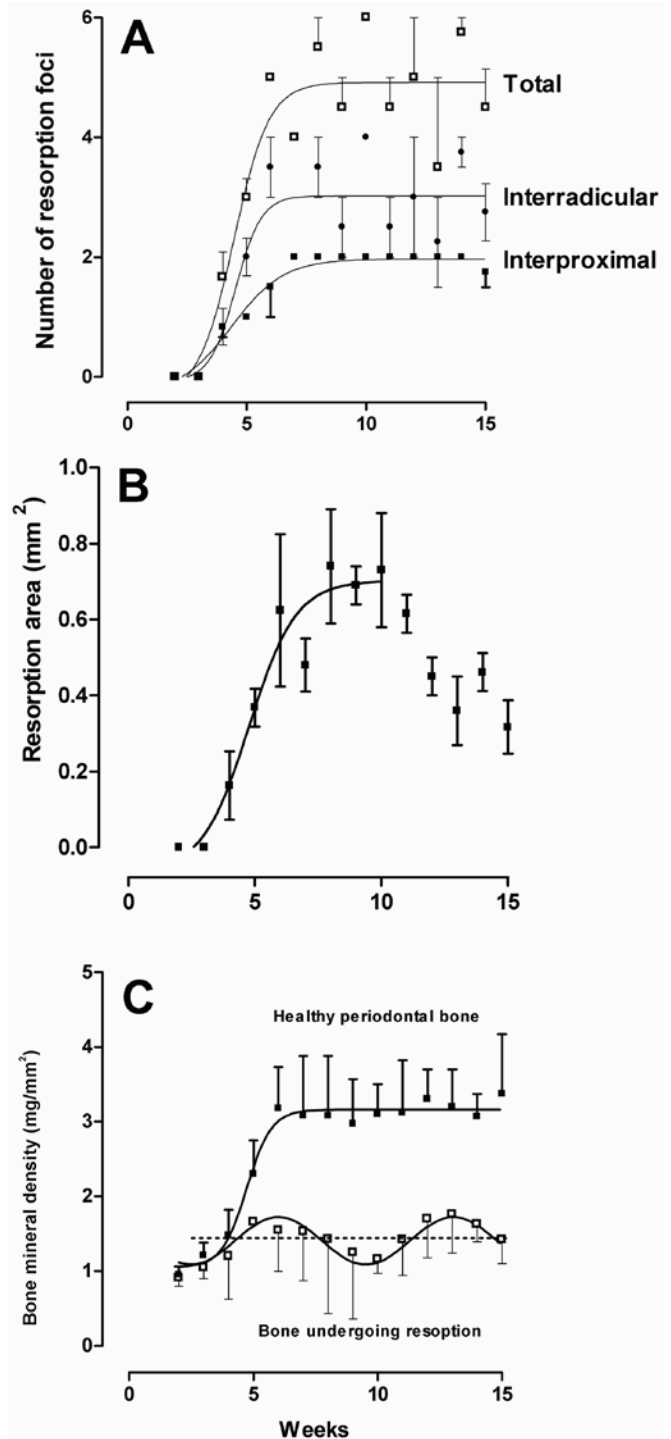


Figure 5. (A) Number of bone resorption areas (interproximal, interradicular, and their sum) as a function of age. (B) Time course of the total area (measured on the lateral projection of the hemimandible) undergoing bone resorption, as a function of age. (C) Time course of the calcification of healthy periodontal bone (solid squares) and of focal resorption areas as a function of age. Data are given as the mean \pm SE of 4 to 6 animals per point.

In general, growth curves contain an age t' at which the growth rate changes from curving upward (increasing exponentially) to curving downward (following the law of diminishing returns). As a consequence the function has a POI at t' , when the growth rate is maximum. Biologists refer to growth at its maximum rate as the growth spurt. There is general consensus that various radical physiologic changes are occurring at the POI. For example,

t' can mark sexual maturation, when the animal changes from the vegetative to the procreative phase.⁶ An alternative view is that before the POI, anabolic processes in the body are of greater intensity than the catabolic ones; the opposite occurring after the POI.⁵ On these grounds, we use the POI of the function fitting the data of a periodontal process to qualify it as either independent or associated with the body growth process.

The growth and development of the animals involved in the current study, assessed with the Parks law of ad libitum feeding and growth,¹⁷ have been published elsewhere.¹⁸ Use of the Parks equation requires weekly measurements of body weight and food intake. Because it does not require measurement of food intake, we used the Boltzmann equation to estimate the POIs of periodontal processes. The fact that the dry weight of the hemimandible exhibited a POI at 5.8 ± 2.2 wk ($n = 43$), strongly suggests that overall hemimandibular growth is harmonic with body growth (7 ± 1 wk¹⁸).

As reported in the literature,¹¹ the presence of hair or bedding material at the most-coronal portions of the papilla or within the epithelium and the subepithelial connective tissue of gnotobiotic rats is the cause of nonbacterial periodontal disease. In contrast, our histologic review revealed no evidence of this phenomenon, indicating that keeping young rats in hanging wire cages under strict hygienic conditions successfully avoided that confounding factor in this population.

Characteristics of the molar teeth and mastication. Because rats have single dentition, the diameter of molar teeth remained constant throughout their lives. The mineral density of the crowns of the first and second molars, measured in the vestibular-lingual projection, increased as a function of time with similar rates and asymptotes. Irrespective of the age of the animal, matrices mature and mineralize after their synthesis.²⁵ Eruption of the first and second molars occurs at the second week of life and cooperates with the intake of solid food at this stage. The third molar, on the other hand, erupts at the fourth week of age, when the animals are weaned and receive solid food.

In an alternative explanation for the different characteristics of the third molar, the mandible can be considered a simple, sagittally oriented second-class lever, with the jaw joint as a fulcrum.²⁶ This disposition decreases the force needed to ground hard food by a factor of 3 or 4. The progressive reduction in diameter of first to third molar teeth progressively increases in the pressure exerted on food particles at occlusion. The higher mineral content of the third molar can be interpreted as an improvement in the ability to chew foods of different degrees of hardness.

Measurement of periodontal bone support. The rate of tooth eruption is always faster than the concomitant rate of bone apposition at the alveolar crest.⁴ The occlusobuccally erupting and distally shifting molars emerge from their sockets over time and, as a consequence, the distance between the alveolar bone crest and cemento enamel junction increases. Evidence suggests that molars continue to erupt and the alveolar process continues to grow in height throughout most of a rodent's life.¹ As expected, the hardness of food caused erosion of occlusal surfaces and the height of the length occlusocervical surface of molar crowns decreased as a function of time (Figure 3 A). In our rats eruption approached its asymptote at approximately 15 wk of age. Two well-known phenomena affect periodontal bone support: active eruption beginning at 2 wk of age and passive eruption produced by apposition of cement at the root apex, which compensates for attrition of occlusal surfaces (Figure 3 B, upper curve). Periodontal bone disease, if present, is a third phenomenon that has to be considered. Correct estimation of periodontal bone support requires that measurement of the

distance between the cemento enamel junction and alveolar bone crest is corrected for the height of bone resorption area to account for this transient bone resorption phenomenon.

Rat molar teeth erupt concurrent with a high rate of bone turnover, characteristic of the most active period of growth.¹⁸ The rate of growth of the distance between the cemento enamel junction and alveolar bone crest (Figure 3A, lower curve) was significantly ($P = 0.0001$) slower than that of growth in the height of resorption areas (Figure 3A, upper curve). Although the junction-to-apex variable approached its asymptote at 15 wk, that for the resorption variable occurred at approximately 10 wk. The differences in the rates of growth of these 2 variables explain the biphasic character of periodontal bone support as a function of age (Figure 3 B).

Distance between the cemento enamel junction and alveolar bone crest. The overall results of our current study agree with those obtained previously.¹ The kinetics regarding the distance between the cemento enamel junction and alveolar bone crest agreed with those for body growth. In addition, the joint-to-crest distance increased with age and was larger on the lingual than vestibular view (Figure 4). On the lingual view, the data fitted a sigmoidal function with a POI that did not differ significantly from that of body growth. We conclude that the joint-to-crest distance is associated with body growth in young control rats. The data from the vestibular view did not converge to the sigmoidal function, probably because of large experimental errors regarding the lengths measured and number of observations. Several theories regarding the differences between the lingual and vestibular growth kinetics have been proposed.

Statistically significant differences in modeling and remodeling activities occur at the buccal and lingual plates of alveolar bone in control animals. In a description of the physiologic drift of rat molar teeth in correlation with growth of the maxilla and mandible,²² apposition of bone along the mesial alveolar wall and resorption of the bone along the distal wall were characteristic for all the molar teeth. In particular, distal drift was an intermittent phenomenon, as shown by cyclic reparative apposition of bone on the resorbed surfaces with alternating disorganization and reorganization of the periodontal membrane. Further, the molar teeth not only tilt mesially while migrating distally, they also tilt lingually and slightly buccally,⁴ perhaps as a consequence of the daily load imposed by the demands of feeding on the bone structure of the mandible and jaw.

In addition, the lingual plate erodes due to feeding.³⁰ Incised food particles are transported toward the molars by means of coordinated jaw and tongue movements. The prominent palatal rugae of the diastemal region facilitate this process. The lingual components may enhance grinding efficiency, particularly during the anterior power stroke. A movable symphysis appears to be of critical importance in facilitating this type of mastication.

Rate of mineral acquisition. The rate of mineral acquisition by the hemimandible followed a sigmoidal trace with a POI consistent with that of body bone mass.¹⁸

Transient periodontal bone resorption in young rats. X-ray densitometry yields a high ratio of quality of information to cost, given the small volume of periodontal bone (approximately 18 mm³ at 15 wk of age, 7% of total hemimandibular volume) involved and the excellent quality of the digital images obtained. Our X-ray densitometric studies revealed transient periodontal bone resorption, a phenomenon that receded spontaneously. Alveolar bone is unique in its increased rate of metabolism, which for any given age, exceeds that of diaphyses of long bones.²⁰ Alveolar bone is in a constant state of flux with regard

to height, contour, and density in response to forces exerted upon it. As a tooth migrates, the lingual side of the socket is in continuous bone formation, whereas the opposite side shows cyclic resorption and formation within small foci.^{10,27} The use of dynamic histomorphometric techniques have shown that the remodeling cycle lasts 6 d (1.5 d for bone resorption, 3.5 d for reversal, and 1 d formation),²⁹ thus explaining the permanent instability of alveolar bone.³¹

The kinetics of the overall bone resorption phenomenon was assessed in the current study through the sum of radiolucent areas observed in radiographs of the hemimandibles. The POI of this variable occurred at 4.5 ± 0.6 wk, significantly earlier ($P = 0.035$) than the POI for overall growth (7 ± 1 wk).¹⁸ Because the osteoclasts counts in alveolar bone did not increase between 3 and 9 wk of age, the sinusoidal time course of bone mineral density at the resorption areas is consistent with the reported intense metabolic activity of periodontal bone tissue²⁹ and focused our attention on nonosteoclastic bone resorption.

Osteoclastic activities depending on matrix metalloproteinases contribute prominently to bone matrix solubilization in specific areas of the skeleton and in some developmental and pathological situations.⁸ The fact that none of the matrix metalloproteinases identified in osteoclasts thus far appear limiting for resorption supports the hypothesis that the critical enzyme for bone solubilization is produced by nonosteoclastic cells.¹² The fibroblast-like cells that develop at the bone surface during aseptic prosthesis loosening are capable of resorbing bone without the help of osteoclasts.¹⁶ These fibroblasts acquire their ability to degrade bone early during differentiation and, on stimulation, release acidic components that lower the pH of their pericellular milieu. In vitro, the secretion products of these fibroblasts were active in degrading dentin, albeit at a lower rate (that is, 17% to 50%) than that of osteoclasts under similar experimental conditions. In agreement with these data, cells harvested from bone marrow, cultured in vitro, and expressing a monocyte-macrophage phenotype (but not osteoclastic markers) can cause bone resorption.²⁴ The amassed information suggests that monocytes-macrophages play a direct role in osteolysis through cathepsin-K-associated proteolytic degradation of bone matrix. Whether nonosteoclastic resorption occurs at the periodontium of growing rats and participates in the adaptation of periodontal structures during the growth period requires further research.

Acknowledgments

This work was supported by grant CONICET PIP5018 from the Consejo Nacional de Investigaciones Científicas y Técnicas. RCP, AR, and HM are Research Career Members of the Consejo Nacional de Investigaciones Científicas y Técnicas.

References

- Amstad-Jossi M, Schroeder HE. 1978. Age-related alterations of periodontal structures around the cemento-enamel junction and of the gingival connective tissue composition in germfree rats. *J Periodontol Res* 13:76–90.
- Baer PN, Newton WL. 1959. The occurrence of periodontal disease in germfree mice. *J Dent Res* 38:1238.
- Baer PN, Newton WL. 1960. Studies on periodontal disease in the mouse. III. The germfree mouse and its conventional control. *Oral Surg Oral Med Oral Pathol* 13:1134–1144.
- Belting CM, Schour I, Weinman JP, Shepro MJ. 1953. Age changes in the periodontal tissues of the rat molar. *J Dent Res* 32:332–353.
- Bertalanffy L. 1957. Quantitative laws in metabolism and growth. *Q Rev Biol* 32:217–231.
- Brody S. 1974. Bioenergetics and growth. New York (NY): Hafner Press.
- Calderari S, Font MT, Garroco O, Martínez SM, Morini JC, Puche RC, Tarrés MC. 1991. The inbred IIM/Fm stock. *Rat News Lett* 25:28–29.
- Delaissé JM, Andersen TL, Engsig MT, Henriksen K, Troen T, Blavier L. 2003. Matrix metalloproteinases (MMP) and cathepsin K contribute differently to osteoclastic activities. *Microsc Res Tech* 61:504–513.
- Falconer D, Mackay T. 1996. Introduction to quantitative genetics, 4th ed. New York (NY): Longman.
- Gorustovich AA, Steimetz T, Giglio MJ, Guglielmotti MB. 2006. A histomorphometric study of alveolar bone modeling and remodeling under experimental anaemia and polycythaemia in rats. *Arch Oral Biol* 51:246–251.
- Heijl L, Wennström J, Lindhl J, Socransky SS. 1980. Periodontal disease in gnotobiotic rats. *J Periodontol Res* 15:405–419.
- Hou P, Troen T, Ovejero MC, Kirkegaard T, Andersen TL, Byrjalsen I, Ferreras M, Sato T, Shapiro SD, Foged NT, Delaissé JM. 2004. Matrix metalloproteinase 12 (MMP12) in osteoclasts: new lesson on the involvement of MMPs in bone resorption. *Bone* 34:37–47.
- Klausen B, Todd Evans R, Sfintescu C. 1989. Two complementary methods of assessing periodontal bone level in rats. *Scand J Dent Res* 97:494–499.
- Meema HE, Harris CK, Porret RE. 1964. A method for determination of bone-salt content of cortical bone. *Radiology* 182:986–997.
- Page RC, Schroeder HE. 1982. Periodontitis in man and other animals. Basel (Switzerland): Karger.
- Pap T, Claus A, Ohtsu S, Hummel KM, Schwartz P, Drynda S, Pap G, Machner A, Stein B, George M, Gay RE, Neumann W, Gay S, Aicher WK. 2003. Osteoclast-independent bone resorption by fibroblast-like cells. *Arthritis Res Ther* 5:R163–R173.
- Parks JR. 1982. A theory of feeding and growth of animals. Berlin (Germany): Springer Verlag.
- Puche RC, Alloati R, Ledesma S. 1988. Growth and development of the bone mass of two strains of inbred rats. *Bone Miner* 4:341–353.
- Rasband W. 2008. NIH Image [Internet]. Available at <http://reb.info.nih.gov/nih-image/manual/contents.html>.
- Rogers HJ, Weidman SM. 1951. Metabolism of alveolar bone. *Br Dent J* 90:7–10.
- Saffar JL, Lasfargues JJ, Cherruau M. 1997. Alveolar bone and the alveolar process: the socket is never stable. *Periodontol* 2000 13:76–90.
- Sicher H, Weinmann JP. 1944. Bone growth and physiologic tooth movement. *Am J Orthod Oral Surg* 30:C109–C119.
- Snedecor GW, Cochran CW. 1976. Statistical methods. Ames (IA): Iowa State University Press.
- Tamaki Y, Sasaki K, Sasaki A, Takakubo Y, Hasegawa H, Ogino T, Kontinen YT, Salo J, Takagi M. 2008. Enhanced osteolytic potential of monocytes/macrophages derived from bone marrow after particle stimulation. *J Biomed Mater Res B Appl Biomater* 84:191–203.
- Termine JD. 1993. Bone matrix proteins and the mineralization process, p 21–25. In: Favus MJ, editor. Primer on the metabolic bone diseases and disorders of mineral metabolism. New York (NY): Raven Press.
- Turnbull WS. 1970. Mammalian masticatory apparatus. In: Fieldiana. Geology, vol 18, p 149–356. Chicago (IL): Field Museum Press.
- Ubios AM, Guglielmotti B, Steimetz T, Cabrini RL. 1991. Uranium inhibits bone formation in physiologic alveolar bone modeling and remodeling. *Environ Res* 54:17–23.
- Institute of laboratory Animal Resources. 1996. Guide for the care and use of laboratory animals. Washington (DC): National Academies Press.
- Vignery A, Baron R. 1980. Dynamic histomorphometry of alveolar bone remodelling in the adult rat. *Anat Rec* 196:191–200.
- Weijjs WA. 1975. Mandibular movements of the albino rat during feeding. *J Morphol* 145:107–124.